Supplemental material to this article can be found at:
http://molpharm.aspetjournals.org/content/suppl/2021/11/11/molpharm.121.000365.DC1
1521-0111/101/1/13–23$35.00 https://doi.org/10.1124/molpharm.121.000365
MOLECULAR PHARMACOLOGY Mol Pharmacol 101:13–23, January 2022
Copyright © 2021 by The American Society for Pharmacology and Experimental Therapeutics

Chrysosplenol-C Increases Contraction by Augmentation of Sarcoplasmic Reticulum Ca^{2+} Loading and Release via Protein Kinase C in Rat Ventricular Myocytes[S]

J. Wang, T.N. Trinh, A. T. V. Vu, J.C. Kim, A.T.N. Hoang, C.J. Ohk, Y.H. Zhang, C.M. Nguyen, and S.H. Woo

Pathophysiology Laboratory, College of Pharmacy, Chungnam National University, Yuseong-gu, Daejeon, South Korea (J.W., T.N.T., A.T.V.V., S.H.W.); NEXEL Co., Ltd. 8F, 55 Magokdong-ro, Gangseo-gu, Seoul, South Korea (J.C.K.); Institute of Natural Products Chemistry, VAST, Hanoi, Vietnam (A.T.N.H., C.M.N.); and Department of Physiology and Biomedical Sciences, College of Medicine, Seoul National University, Jongro-gu, Seoul, South Korea (C.J.O., Y.H.Z.)

Received July 8, 2021; accepted October 11, 2021

ABSTRACT

Naturally found chrysosplenol-C (4′,5,6-trihydroxy-3,3′,7-trimethoxyflavone) increases the contractility of cardiac myocytes independent of β-adrenergic signaling. We investigated the cellular mechanism for chrysosplenol-C–induced positive inotropy. Global and local Ca^{2+} signals, L-type Ca^{2+} current (I_{Ca}), and contraction were measured from adult rat ventricular myocytes using two-dimensional confocal Ca^{2+} imaging, the whole-cell patch-clamp technique, and video-edge detection, respectively. Application of chrysosplenol-C reversibly increased Ca^{2+} transient magnitude with a maximal increase of ~55% within 2- to 3-minute exposures ($EC_{50} \cong 21$ μM). This chemical did not alter I_{Ca} and slightly increased diastolic Ca^{2+} level. The frequency and size of resting Ca^{2+} sparks were increased by chrysosplenol-C. Chrysosplenol-C significantly increased sarcoplasmic reticulum (SR) Ca^{2+} content but not fractional release. Pretreatment of protein kinase C (PKC) inhibitor but not Ca^{2+}/calmodulin-dependent protein kinase II (CaMKII) inhibitor abolished the stimulatory effects of chrysosplenol-C on Ca^{2+} transients and Ca^{2+} sparks. Chrysosplenol-C–induced positive inotropy was removed by the inhibition of PKC but not CaMKII or phospholipase C. Western blotting assessment revealed that PKC-δ protein level in the membrane fractions significantly increase within 2 minutes after chrysosplenol-C exposure with a delayed (5-minute) increase in PKC-α levels in insoluble membrane. These results suggest that chrysosplenol-C enhances contractility via PKC (most likely PKC-δ)-dependent enhancement of SR Ca^{2+} releases in ventricular myocytes.

SIGNIFICANCE STATEMENT

Study shows that chrysosplenol-C, a natural flavone showing a positive inotropic effect, increases SR Ca^{2+} releases on depolarizations and Ca^{2+} sparks with an increase of SR Ca^{2+} loading but not L-type Ca^{2+} current in ventricular myocytes. Chrysosplenol-C–induced enhancement in contraction is eliminated by PKC inhibition, and it is associated with redistributions of PKC to the membrane. These indicate that chrysosplenol-C enhances contraction via PKC-dependent augmentations of SR Ca^{2+} release and Ca^{2+} loading during action potentials.

Introduction

Chrysosplenol-C (4′,5,6-trihydroxy-3,3′,7-trimethoxyflavone) is a flavonoid compound contained in the medicinal plants *Pterocaulon sphacelatum* (Asteraceae) (Semple et al., 1999) and *Miliusa balansae* (Huong et al., 2004). It is known that *M. balansae* in particular has therapeutic effects for gastropathy and glomerulonephropathy. We have previously demonstrated that chrysosplenol-C increases cell shortening in rat ventricular myocytes (EC_{50} of ~45 μM; Son et al., 2011). The positive inotropic effect of chrysosplenol-C was reversible and resistant to the inhibitors for β-adrenergic receptor and protein kinase A (PKA) (Son et al., 2011). The cellular mechanism for the chrysosplenol-C–induced positive inotropic effect remains to be determined.

The contraction of mammalian cardiac myocytes is controlled by a sequence of events called excitation-contraction coupling, which includes the L-type Ca^{2+} current (I_{Ca})-triggered gating of the Ca^{2+} release channels, ryanodine receptors (RyRs) on the sarcoplasmic reticulum (SR) membrane, and the release of Ca^{2+} from the SR (Beuckelmann and Wier, 1988; Näbauer et al., 1989; Niggli and Lederer, 1990). Confocal Ca^{2+} imaging of cardiac myocytes has shown that there are elementary SR Ca^{2+} release events via RyRs ("Ca^{2+} sparks") underlying cardiac excitation-contraction coupling that are activated spontaneously or by I_{Ca} (Cheng et al., 1993; Cannell et al., 1994; Shacklock et al.,

This work was supported by National Research Foundation of Korea (NRF) grants funded by the Korean Government (MEST) (2017R1E1A1A01074504).
No author has an actual or perceived conflict of interest with the contents of this article.
dx.doi.org/10.1124/molpharm.121.000365.
[S] This article has supplemental material available at molpharm.aspetjournals.org.

ABBREVIATIONS: τ, decay time constant; CaMKII, Ca^{2+}/calmodulin-dependent protein kinase II; 2-D, two-dimensional; FWHM, full-width at half-maximal amplitude; GAPDH, glyceraldehyde-3-phosphate dehydrogenase; I_{Ca}, L-type Ca^{2+} current; PDBu, phorbol dibutyrate; PKA, protein kinase A; PKC, protein kinase C; PLC, phospholipase C; RyR, ryanodine receptor; SR, sarcoplasmic reticulum.

1995). After the contractile elements are activated, the released Ca^{2+} is removed from the cytosol mainly by the SR Ca^{2+} pump and the forward mode of the Na^+-Ca^{2+} exchanger (Negretti et al., 1993; Bassani et al., 1994).

In addition to PKA, the other key protein kinases Ca^{2+}/calmodulin-dependent protein kinase II (CaMKII) and protein kinase C (PKC) are well known to regulate cardiac Ca^{2+} signaling and myocytes' contractility. These kinases are often involved in the mode of action for positive inotropic agents in cardiac myocytes (Guo et al., 2006; Zhou et al., 2009; Ogrodnik and Niggli, 2010; Kim et al., 2015; Bovo et al., 2017; Steinberg, 2018). Although no role of PKA signaling in chrysosplenol-C–induced positive inotropy has been previously reported (Son et al., 2011), the possible roles of these kinases in the action of chrysosplenol-C remain to be examined. It is thought that Ca^{2+}-dependent CaMKII activation can modulate Ca^{2+}-induced Ca^{2+} release via phosphorylation in a number of excitation-contraction coupling proteins, including L-type Ca^{2+} channels and RyRs (Maier and Bers, 2007). The phosphorylation of RyRs by CaMKII can sensitize RyRs to Ca^{2+}, resulting in an increased SR Ca^{2+} leak (Guo et al., 2006; Pereira et al., 2007). Activation of PKC signaling is involved in positive inotropy and Ca^{2+} modulation under the stimulations of α_1-adrenergic and endothelin receptors in cardiac myocytes, in which there are also significant controversies (Capogrossi et al., 1991; Asai et al., 1996; Woo and Lee, 1999a,b; Braz et al., 2004; Puglisi et al., 2011; Smyrnias et al., 2018).

In the present study, we investigated the cellular mechanisms underlying the positive inotropy of chrysosplenol-C by examining global and local Ca^{2+} signals, I_{Ca}, and contraction in isolated rat ventricular myocytes using confocal Ca^{2+} imaging, the whole-cell patch-clamp technique, and video edge detection, respectively. In addition, the possible role of protein kinases in the effects of chrysosplenol-C has been examined. We find that chrysosplenol-C significantly increases SR Ca^{2+} release upon depolarization, resting Ca^{2+} sparks, and SR Ca^{2+} content and that the stimulatory effects of chrysosplenol-C on Ca^{2+} release sites and contraction are abolished by PKC inhibition. Immunoblotting analysis showed chrysosplenol-C–induced redistribution of PKC subtypes from soluble to the particulate compartment within 2 minutes, which is presumed to represent the activation of PKC. Our data indicate that chrysosplenol-C elicits a positive inotropic effect via PKC (presumably δ subtype)–mediated augmentation in Ca^{2+} signaling in ventricular myocytes.

Materials and Methods

Single Cell Isolation. Ventricular myocytes were isolated from male Sprague-Dawley rats (200–300 g) as described previously (Kim et al., 2015). Rats were deeply anesthetized with sodium pentobarbital (150 mg/kg, i.p.), the chest cavity was opened, and hearts were excised. This surgical procedure was carried out according to the guiding principles for the care and use of experimental animals published by the Korean Food and Drug Administrations and Animal and Plant Quarantine Agency in South Korea and approved by Animal Care and Use Committees of the Chungnam National University (CNU-00368). The excised hearts were retrogradely perfused at 7 ml/min through the aorta (at 36.6°C), first for 3 minutes with Ca^{2+}-free Tyrode's solution composed of (in mM) 137 NaCl, 5.4 KCl, 10 HEPES, 1 $MgCl_2$, and 10 glucose (pH 7.3); then with Ca^{2+}-free Tyrode's solution containing collagenase (1.4 mg/ml, type 1; Roche) and protease (0.14 mg/ml, type XIV; Sigma) for 12 minutes; and finally with Tyrode's solution containing 0.2 mM $CaCl_2$ for 5 minutes. The ventricles of the digested heart were then cut into several sections and subjected to gentle agitation to dissociate the cells. The freshly dissociated cells were stored at room temperature in Tyrode's solution containing 0.2 mM $CaCl_2$.

Two-Dimensional Confocal Ca^{2+} Imaging and Image Analysis. Isolated myocytes were loaded with 3 μM fluo-4 acetoxymethyl ester (Invitrogen, USA) for 30 minutes. The dye-loaded cells were continuously superfused with 2 mM Ca^{2+}-containing normal Tyrode's solution (see above; pH 7.4). Intracellular Ca^{2+} fluorescence was imaged in 2-D using a laser scanning confocal imaging system (A1, Nikon, Japan) attached to an inverted microscope (Eclipse Ti, Nikon) fitted with a ×60 oil-immersion objective lens (Plan Apo, Numerical Aperture 1.4, Nikon). Dyes were excited at 488 nm using Ar ion laser (Ommichrome), and fluorescence emission at >510 nm was detected. Images were recorded by NIS Elements AR software (v3.2, Nikon). To record global Ca^{2+} transients, cells were stimulated at 1 Hz using a pair of Pt electrodes connected to a stimulator (D-7806, Hugo Sachs Elektronik, Germany), and Ca^{2+} images were recorded at 60 or 120 Hz. To estimate the magnitudes of Ca^{2+} transients, the average resting fluorescence intensity (F_0) was calculated from several frames immediately before electrical stimulation, and then tracings of global Ca^{2+} signals were shown as the average fluorescence of each area normalized relative to the F_0 (F/F_0).

To measure spark frequency, Ca^{2+} images were recorded at 30 Hz in 2-D, which allowed us to monitor the major part of the cell and compensate for the scarcity of resting Ca^{2+} sparks. Recording of spontaneous Ca^{2+} sparks was normally preceded by a train of electrical pulses at 1 Hz. Under this condition, the frequency of spontaneous sparks and SR Ca^{2+} content were stable during the experimental period. Ca^{2+} sparks were identified by a computerized algorithm in the "RealTimeMicroscopy" PC program as previously described (Kim et al., 2015). To calculate the frequency of Ca^{2+} sparks, the area of cell image was measured using the NIS Elements AR software (v3.2, Nikon). The focal Ca^{2+} releases were subjected to Gaussian approximations as previously described using the PC program "RealTimeMicroscopy" (Kim et al., 2015), which allowed routine measurements of the amplitude, width, and area of sparks (Fig. 4). Duration of focal Ca^{2+} releases was estimated as the time-to-peak area (Woo et al., 2003).

Measurement of I_{Ca}. I_{Ca} was recorded in the whole-cell configuration of the patch-clamp technique (Hamill et al., 1981) using an EPC7 amplifier (HEKA, Germany). The patch pipettes were made of glass capillaries (Kimble Glass Inc.) to have a resistance of 2–3 MΩ when filled with the internal solution containing (in mM) 110 CsCl, 20 TEA-Cl, 20 HEPES, 5 MgATP, and 15 EGTA, with the pH adjusted to 7.2 with CsOH. Outward K^+ currents were suppressed by replacing internal K^+ with Cs^+ and TEA^+, and inward rectifier K^+ current was suppressed by replacing external K^+ with Cs^+. Na^+ current was inactivated by holding the membrane potential at –40 mV. Trains of test pulses were to 0 mV for 120 milliseconds at 0.1 Hz. The measurement of I_{Ca} was carried out 7–8 minutes after rupture of the membrane with the patch pipette. Generation of voltage protocols and acquisition of data were carried out using pCLAMP (9.0, Molecular Devices) combined with an analog-to-digital converter (Digidata 1322, Molecular Devices). The series resistance was 1.5–5 times the pipette resistance and was electronically compensated through the amplifier. The current signals were digitized at 10 kHz. The percent suppression of I_{Ca} by interventions was evaluated after a gradual decrease in I_{Ca} by rundown was subtracted from the raw current. Peak detection was performed with Clampfit (9.0, Molecular Devices), and the time constant (τ) of inactivation of I_{Ca} was obtained with single exponential curve fitting using the equation: $y = (A_i - A_f) \cdot \exp(-t/\tau) + A_f$, wherein A_i and A_f are the initial ($t = 0$) and final (t = infinity) values of the parameter, and τ is a time constant of exponential decay. Curve fitting was performed using OriginPro 8 SR0 software (OriginLab Corporation).

Measurement of Cell Shortening. Isolated myocytes were continuously superfused with normal Tyrode's solution containing 2 mM Ca^{2+}. Cells were field-stimulated with two paralleled Pt wires connected with an electrical stimulator (Stimulator I Hugo Sach

Elektronik, March-Hugstetten, Germany) at 1 Hz. Single cell shortening was detected with a video edge detector (Model VED-105; Crescent Electronics, Sandy, UT) connected with a CCD camera (LCL902C; Till Photonics, Graefelting, Germany) and video monitor (Polychrome V system; Till Photonics) (Son et al., 2011). Signals from the edge detector were digitized by Digidata (1440A; Molecular Devices, Sunnyvale, CA) and then recorded with pClamp program (v10.3, Molecular Devices).

Subcellular Fractionation and Western Blot Analysis. To examine protein expression levels of PKC isoforms, rat ventricular myocytes were collected and treated with chrysosplenol-C (80 μM) for 2, 5, and 30 minutes. Cells were resuspended in lysis buffer without SDS (10 mM Tris-HCl, 1 mM phenylmethanesulfonyl fluoride, 1 mM Na_3VO_4, 0.5 μM NaF, and protease inhibitors including 0.2 μg/ml pepstatin, 1 μg/ml aprotinin, 0.5 μg/ml leupeptin, pH 7.4), sonicated five times by using a sonicator (Sonopuls, Berlin, Germany) for 2 seconds, and then centrifuged for 30 minutes at 100,000 g to obtain the cytosol. The resulting pellet was resuspended with lysis buffer containing 1% (w/v) SDS and 1% Trition-X 100 and incubated in ice for 30 minutes. Then, the sample was centrifuged at 100,000 g for 30 minutes. The supernatant was the Triton-soluble membrane fraction, and the pellet was considered to be the Triton-insoluble fraction. Protein concentrations were measured by BCA protein assay (Thermo Fisher Scientific, 23227). Approximately 25 μg of proteins was run on 10% SDS-polyacrylamide gel. The proteins were transferred onto a nitrocellulose membrane, and the blots were sequentially probed with primary and secondary antibodies (anti–PKC-α, mouse monoclonal, 1:500, an epitope at the C terminus, sc-8393, Santa Cruz Biotechnology; anti–PKC-δ, mouse monoclonal, 1:500, an epitope at the C terminus, sc-8402, Santa Cruz Biotechnology; anti–PKC-ε, mouse monoclonal, 1:500, an epitope at the C terminus, sc-1681, Santa Cruz Biotechnology; anti–Na^+-K^+ ATPase α2, rabbit polyclonal, 1:500, an epitope at an N terminal, 07-674, Merck; anti-GAPDH, mouse monoclonal, 1:1000, ab8245, Abcam; secondary antibodies: mouse anti-rabbit IgG–horseradish peroxidase, 1:5000, sc-2357, Santa Cruz Biotechnology; goat anti-mouse IgG–horseradish peroxidase, 1:5000, sc-2005, Santa Cruz Biotechnology) using standard Western blot protocol. All blots were imaged using a ChemiDoc XRS densitometer (Bio-Rad) and quantified by Image J program.

Solutions and Reagents. Chrysosplenol-C was isolated from air-dried and ground leaves and branches of *M. balansae* as previously described (Son et al., 2011). The purity of chrysosplenol-C was 98.1 ± 0.99% (three batches). Detailed physicochemical and structural information on chrysosplenol C has been reported previously (Son et al., 2011). Stock solutions of chrysosplenol-C (500 mM) were made in DMSO, and it was diluted in Tyrode solution for testing (DMSO ≤0.08% (v/v), e.g., 0.01% DMSO at 50 μM chrysosplenol-C solutions). Same concentration of DMSO was added to Tyrode solutions without (control solutions and inhibitor-containing solutions) or with chrysosplenol-C. The drug solutions were applied to the cells by superfusion. The experiments were performed at room temperature (22–25°C).

Caffeine, chelerythrine, KN-92 (E)-*N*-(2-(((3-(4-chrolophenyl)allyl) (methyl)amino) methyl)phenyl)-4-methoxybenzenesulfonamide), and KN-93 (2-[*N*-(2-hydroxyethyl)]-*N*-(4-methoxybenzenesulfonyl)amino-*N*-(4-chlorocinnamyl)-*N*-methylbenzylamine) were purchased from Sigma-Aldrich (St. Louis, MO). GF109203X (bisindolylmaleimide I), U73122, and U73343 were supplied by Tocris Bioscience (Avonmouth, Bristol, BS11 9QD). Fluo-4 acetoxymethyl was from Thermo Fisher Scientific (Waltham MA).

Statistics. The numerical results are presented as mean ± S.D. *n* indicates number of cells used. Paired or unpaired Student's *t* tests were used for statistical comparisons of most of the functional data depending on the experiments in single group. For comparison of unitary properties of single sparks, nonparametric Mann-Whitney test was performed (Fig. 4). For the Western blot data, statistical significance among the groups was determined using two-way ANOVA-related measures, with post hoc testing to control for multiple comparisons. *p* values were adjusted for multiple comparisons using Bonferroni correction (see figure legends). The statistical significance was defined using a new *p* value threshold of 0.05/(number of tests) according to Bonferroni correction.

Results

Chrysosplenol-C reversibly and stably enhances ventricular cell shortening (Son et al., 2011). To determine the cellular mechanism for the chrysosplenol-C–induced positive inotropic effect, we examined whether chrysosplenol-C affects Ca^{2+} releases from the SR during depolarizations. Figure 1, A and B shows that chrysosplenol-C (50 μM) reversibly increases cytosolic Ca^{2+} releases during depolarizations. The maximal effect of 50 μM chrysosplenol-C was observed at about 2–3 minutes after exposure. Diastolic Ca^{2+} levels were also slightly but significantly increased by chrysosplenol-C (Fig. 1C). The magnitudes of Ca^{2+} transients were increased by chrysosplenol-C in a concentration-dependent manner with an EC_{50} of 21 ± 3.3 μM (Fig. 1D). Maximal effect on the Ca^{2+} transient magnitude (by ≅58% increase) by chrysosplenol-C was achieved at ∼80 μM. Concentration dependence of the effects of chrysosplenol-C on Ca^{2+} transients was slightly lower than that of its positive inotropic effects (≅45 μM) that were previously observed in rat ventricular myocytes (Son et al., 2011). The decay speed of Ca^{2+} transients was not altered by the application of chrysosplenol-C (Fig. 1E). These results suggest that chrysosplenol-C increases depolarization-induced SR Ca^{2+} release, thereby causing an increase in contraction.

Ca^{2+} releases on depolarization are controlled by the Ca^{2+} influx through L-type Ca^{2+} channels (Beuckelmann and Wier, 1988; Näbauer et al., 1989; Niggli and Lederer, 1990). To understand the mechanism for the enhanced Ca^{2+} transients with the treatment of chrysosplenol-C, we next examined the effects of chrysosplenol-C on I_{Ca}. Figure 2 shows the effects of 50- and 80-μM chrysosplenol-C on the whole-cell I_{Ca}. The I_{Ca} was not significantly altered by either concentration of chrysosplenol-C (Fig. 2A). We only observed a gradual rundown during the application of chrysosplenol-C, with no changes in its current-voltage relationship (Fig. 2B) or inactivation time constants (Fig. 2C). This result suggests that chrysosplenol-C–induced enhancement in Ca^{2+} transients may be mediated by I_{Ca}-independent mechanisms.

An increased SR Ca^{2+} release in the presence of chrysosplenol-C may be reflective of a higher propensity of RyR clusters to activate at a given Ca^{2+} concentration through changes in their Ca^{2+} sensitivity. The occurrence and size of Ca^{2+} sparks at rest represent the changes in Ca^{2+} sensitivity and altered properties of Ca^{2+} release through the Ca^{2+} release sites. Therefore, we assessed the effects of chrysosplenol-C on the spatiotemporal properties of spontaneous Ca^{2+} sparks. The treatment of chrysosplenol-C significantly increased the spark frequency (events/[10^3 $\mu m^2 \cdot s$]) in a concentration-dependent manner (EC_{50} = 0.79 ± 0.24 μM; Fig. 3). At 50 μM, it increased the spark frequency by approximately 2-fold (Fig. 3B).

In the next series of experiments, the unitary properties of Ca^{2+} sparks were measured before and after the application of chrysosplenol-C using 2-D Ca^{2+} imaging at 240 Hz. Representative images of spark growth and dissipation in the presence and absence of chrysosplenol-C (50 μM) are shown in Fig. 4. A Gaussian fitting to measure the time course of spark amplitude, width, and area (Fig. 4B; see Materials and Methods) showed

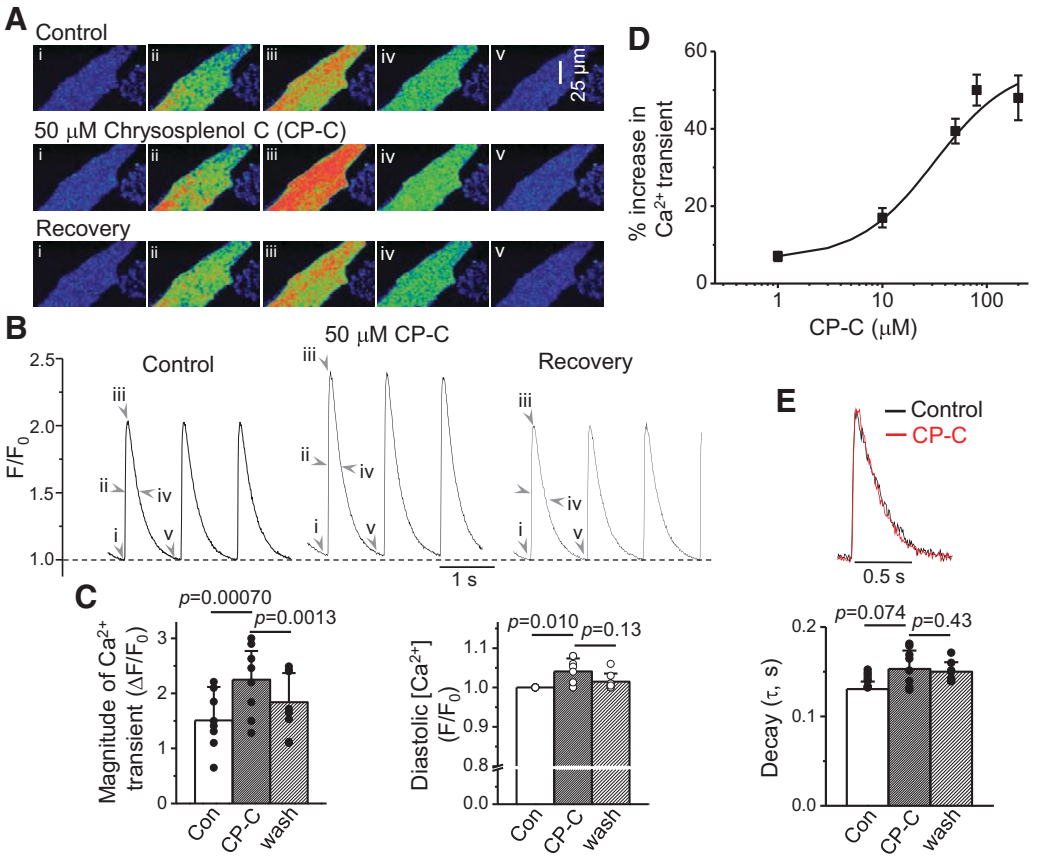

Fig. 1. Enhancement of Ca^{2+} transients by chrysosplenol-C in rat ventricular myocytes. (A) 2-D confocal Ca^{2+} images recorded (120 Hz) from a representative myocyte at the time points marked by Roman numbers with arrowheads in the Ca^{2+} transient traces in (B). (B) Ca^{2+} transients measured from the series of confocal Ca^{2+} images before and after 2-minute chrysosplenol-C (CP-C) (50 μM) exposure. (C) Summary of the effects of CP-C (50 μM) on the Ca^{2+} transient magnitude and diastolic Ca^{2+} level (n = 8). p values obtained from paired t tests were written above the bar graphs. (D) Concentration-response curve for the stimulatory effect by CP-C on the Ca^{2+} transients (% increase) (1 μM, n = 5; 10 μM, n = 5; 50 μM, n = 23; 80 μM, n = 8; 200 μM, n = 5). The curve was approximated by the Hill equation ($y = y_{start} + (y_{end} - y_{start})(x^n/(k^n+x^n))$). EC_{50} (k) = 21 ± 3.3 μM. Max = 57.9 ± 8.59%. (E) Upper: superimposed Ca^{2+} transient traces recorded in the absence and presence of 50 μM CP-C after normalization to their peaks. Lower: summary of the effects of CP-C (50 μM) on the decay time constant (n = 8). Considering the new p value after the Bonferroni correction, p value less than 0.017 (0.05/3 t tests; equivalent to old 0.05) was considered to be significant. Con, control.

that Ca^{2+} spark amplitude slightly increased with no statistical significance after chrysosplenol-C treatment (control: median = 1.64, 90% range = 1.00–2.71; chrysosplenol-C: median = 1.76, 90% range = 0.88–2.15; P = 0.041), whereas the spark width (FWHM, measured at peak area) was unaltered by chrysosplenol-C (control: median = 1.64 μm, 90% range = 1.01–2.23 μm; chrysosplenol-C: median = 1.68 μm, 90% range = 0.93–2.24 μm; P = 0.759; Fig. 4, B and C). The peak area of Ca^{2+} sparks was significantly increased by chrysosplenol-C (control: median = 3.98 μm^2, 90% range = 1.47–8.56 μm^2; chrysosplenol-C: median = 5.10 μm^2, 90% range = 1.44–9.32 μm^2; P = 0.0056). The release durations for individual sparks were not significantly increased by chrysosplenol-C (control: median = 8 milliseconds, 90% range = 4–12 milliseconds; chrysosplenol-C: median = 8 milliseconds, 90% range = 4–16 milliseconds; P = 0.049) (Fig. 4, B and C). These results suggest that chrysosplenol-C increases the amount of Ca^{2+} released from the release sites.

An increase of Ca^{2+} in the lumen of the SR can enhance not only the frequency of Ca^{2+} sparks but also the effectiveness of a given Ca^{2+} current to activate SR Ca^{2+} release (Han et al., 1994; Bassani et al., 1995; Janczewski et al., 1995; Satoh et al., 1997; Györke and Györke, 1998). Therefore, we further examined whether chrysosplenol-C affects SR Ca^{2+} loading by measuring caffeine (10 mM)-induced Ca^{2+} transients. The magnitudes of caffeine-induced Ca^{2+} transients were increased by 50 μM chrysosplenol-C (for 2–3 minutes) to ~135% with increases of Ca^{2+} transient magnitudes (Fig. 5, A and B). The fractional release representing the amount of Ca^{2+} release relative to SR Ca^{2+} content (Bassani et al., 1995) was further calculated as the ratio of the Ca^{2+} transient magnitude during electrical stimulation relative to the magnitude of caffeine-induced Ca^{2+} transients. The fractional release was not significantly changed by chrysosplenol-C (Fig. 5B). The τ of caffeine-induced Ca^{2+} transients were not significantly altered by chrysosplenol-C (Fig. 5B, right). These results suggest that enhancements in Ca^{2+} spark occurrence and Ca^{2+} transients in the presence of chrysosplenol-C may be caused by an increase in SR Ca^{2+} content.

Chrysosplenol-C–induced positive inotropy has been demonstrated to be independent of β-adrenoceptor–PKA signaling (Son et al., 2011). We further examined whether other major kinases, including PKC and CaMKII, play a role in the enhancement of Ca^{2+} transients and Ca^{2+} sparks in the presence of chrysosplenol-C. Interestingly, when the PKC was suppressed by the treatment of chelerythrine (2 μM, 5–10 minute), the application of chrysosplenol-C no longer increased

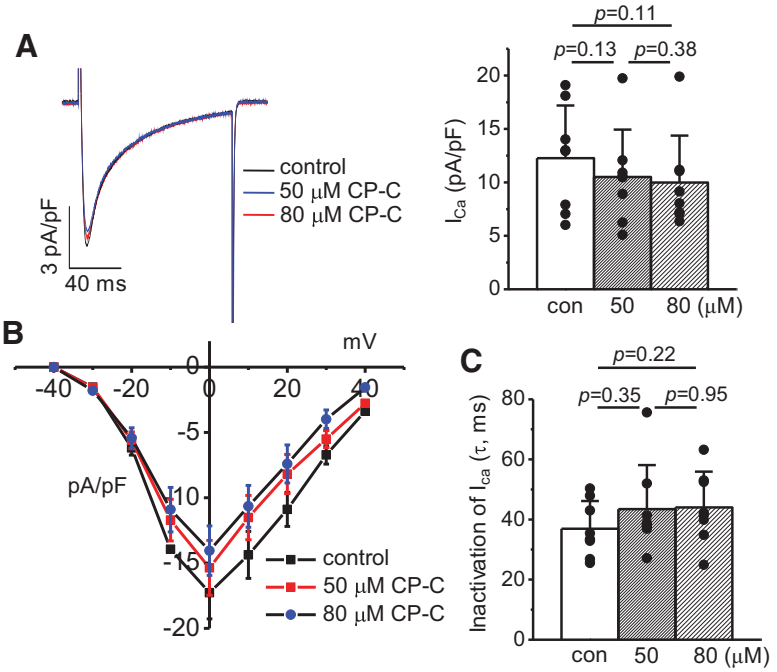

Fig. 2. No effect by chrysosplenol-C on I_{Ca}. (A) Left: superimposed I_{Ca} recorded in the absence and presence of 50 and 80 μM chrysosplenol-C (CP-C) in a representative rat ventricular myocyte. I_{Ca} was recorded on depolarizing pulses from –40 to 0 mV at 0.1 Hz. Right: comparison of averaged I_{Ca} recorded under control condition and after the application of 50 and 80 μM CR-C (n = 8). (B) Averaged current-voltage relationships obtained in the absence and presence of 50 and 80 μM CP-C (n = 6). The currents were recorded during the voltage steps from –40 to +40 mV with 10-mV increment. Holding potential was –40 mV. (C) Averaged inactivation time constants of I_{Ca} measured under the control conditions and after the application of 50 and 80 μM CP-C (n = 8). The p values obtained from paired t tests were written above the bar graphs. con, control.

Ca^{2+} transients (Fig. 6, A and B). Chelerythrine alone did not significantly alter the Ca^{2+} transients (Fig. 6, A and B) or SR Ca^{2+} content (Supplemental Fig. 1). Since PKC can activate CaMKII (Waxham and Aronowski, 1993), the stimulatory effects of chrysosplenol-C may be mediated by CaMKII, activated by PKC. To test this possibility, we examined the effects of chrysosplenol-C on Ca^{2+} transient in the presence of KN-93, the CaMKII inhibitor. Previous reports have shown that KN-93 at a concentration of 1 μM successfully eliminates CaMKII-dependent cardiac Ca^{2+} response (Lu et al., 2020). When this protocol to suppress CaMKII was used in rat ventricular myocytes, chrysosplenol-C (50 μM) slightly increased

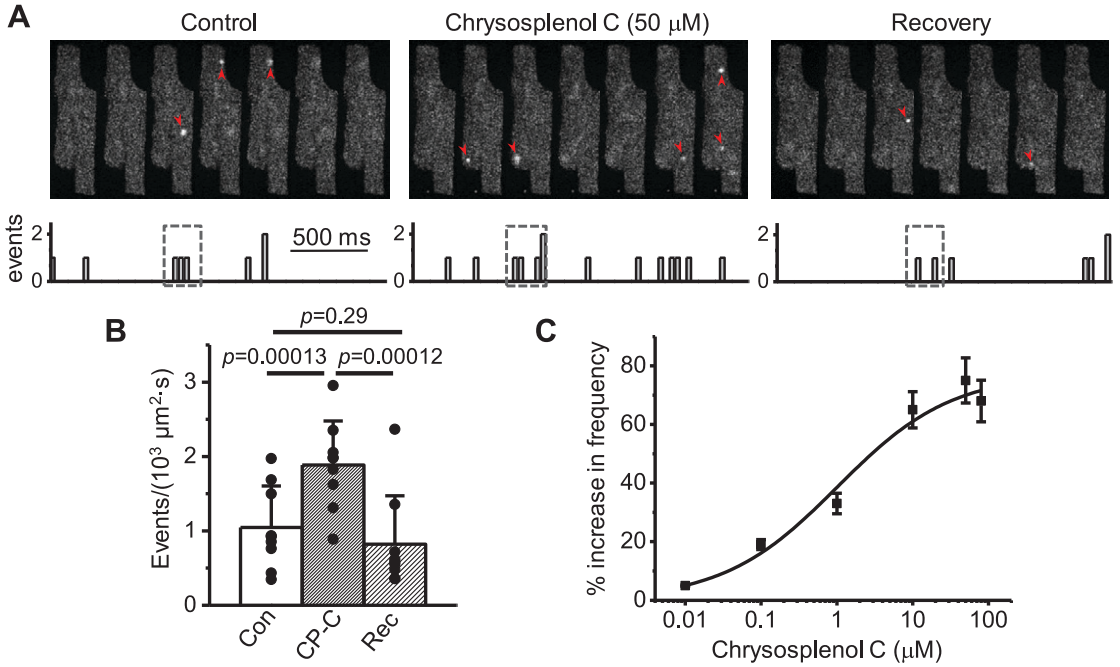

Fig. 3. Enhancement of Ca^{2+} spark occurrence by chrysosplenol-C in rat ventricular myocytes. (A) Upper: 2-D confocal Ca^{2+} images recorded for the period marked by the boxes in the lower panel. Lower: time course of Ca^{2+} spark occurrence per frame for 2-second recording period before and after treatment of chrysosplenol-C (CP-C; 50 μM, 2 minutes). (B) Comparison of mean spark frequency measured in the absence and presence of CP-C (50 μM). $^{***}P < 0.001$ vs. control, $^{\#\#\#}P < 0.001$ vs. CP-C (n = 9; paired t test). The p values obtained from paired t tests were written above the bar graphs. (C) Concentration-response (% increase) curve for the stimulatory effects by CP-C on the resting spark frequency (0.01 μM, 0.1 μM, and 1 μM: n = 5; 10, 50 and 80 μM: n = 8). The curve was approximated by the Hill equation ($y = V_{max} \bullet x^n/(k^n + x^n)$). EC_{50} (k) = 0.79 ± 0.24 μM. Hill coefficient (n) = 0.57 ± 0.06. Con, control; Rec, recovery.

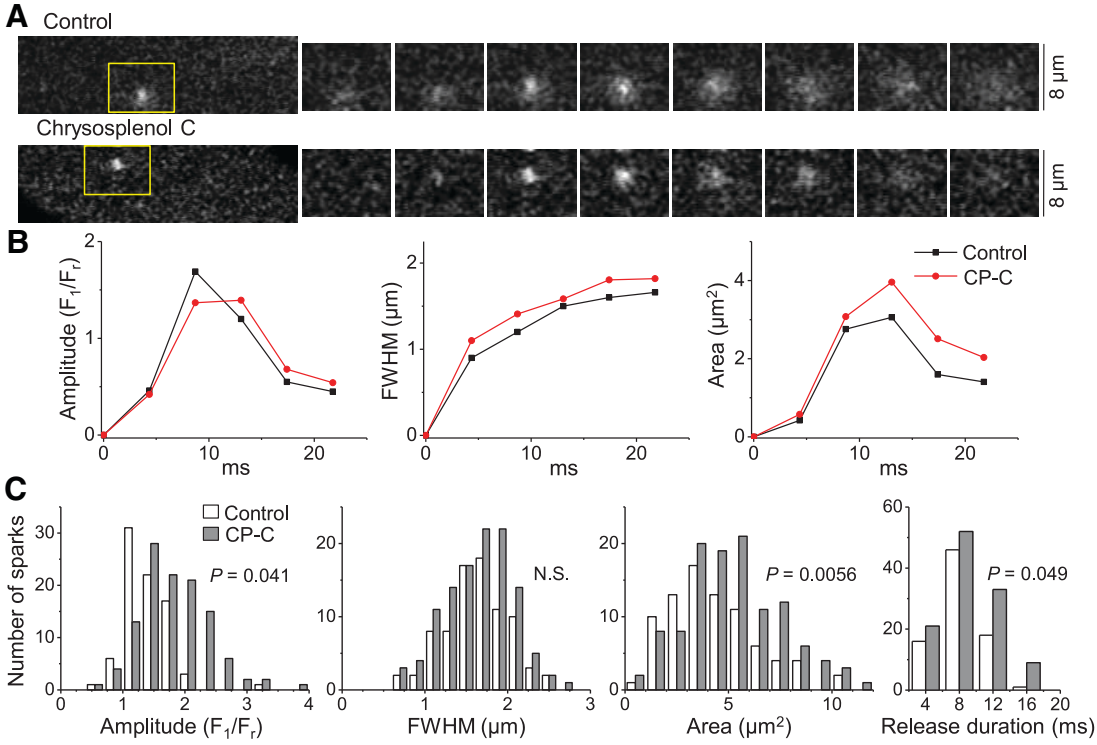

Fig. 4. Effects of chrysosplenol-C on the unitary properties of Ca^{2+} sparks. (A) 2-D confocal Ca^{2+} images for representative Ca^{2+} sparks recorded under control condition and after 2-minute application of chrysosplenol-C (CP-C) (50 μM). Images were recorded at 240 Hz. (B) Time courses of amplitude, full-width at half-maximal amplitude (FWHM) and area of Ca^{2+} spark images shown in the (A) in the absence and presence of CP-C. (C) Distribution histograms for the peak amplitude, FWHM at the time showing peak area, and time-to-peak of area (release duration) of individual Ca^{2+} sparks in the absence and presence of CP-C (50 μM). The Mann-Whitney test was used to evaluate the significant difference between control sparks (n = 81) and sparks recorded in the presence of CP-C (n = 115). Considering the new p value after the Bonferroni correction, p value less than 0.0125 (0.05/4 t tests; equivalent to old 0.05) was considered to be significant.

Ca^{2+} transients with no statistical difference (16 ± 2.2%, n = 9, Fig. 6, C and D). Diastolic Ca^{2+} level was not altered by chrysosplenol-C in the presence of chelerythrine or KN-93 (Table 1). There were no significant changes in the decay time constants of the Ca^{2+} transients recorded in the presence of these blockers with and without chrysosplenol-C (Table 1).

We next tested whether chelerythrine or KN-93 alters the stimulatory effects of chrysosplenol-C on the spark frequency. Treatment with chelerythrine (2 μM) alone did not significantly change the spark frequency (Fig. 6, E and F), whereas KN-93 (1 μM) alone significantly decreased it in the resting ventricular myocytes (by 56 ± 8.8%, n = 8, $P < 0.01$; Fig. 6, G and H). Note that KN-93 alone at the concentrations used significantly reduced the caffeine-induced Ca^{2+} releases (Supplemental Fig. 1). In the myocytes preincubated with chelerythrine, chrysosplenol-C failed to enhance spark occurrence

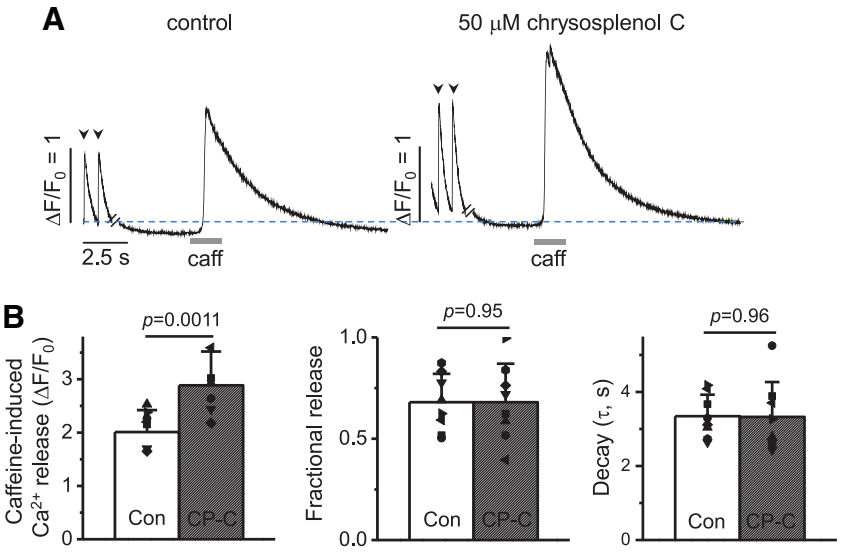

Fig. 5. Increase in SR Ca^{2+} loading with similar fractional release in the presence of chrysosplenol-C (CP-C). (A) Ca^{2+} transients on depolarizations followed by 10 mM caffeine (caff)-induced Ca^{2+} transient measured in the same rat ventricular myocyte in the absence [control (Con)] and presence of CP-C (50 μM, 3 minutes). (B) Mean magnitude of caffeine-induced Ca^{2+} releases representing SR Ca^{2+} content (left), mean fractional release (middle), and mean τ of caffeine-induced Ca^{2+} transients (right), measured before and after application of CP-C in rat ventricular myocytes (n = 8; paired t test). Considering the new p value after the Bonferroni correction, p value less than 0.017 (0.05/3 t tests; equivalent to old 0.05) was considered to be significant.

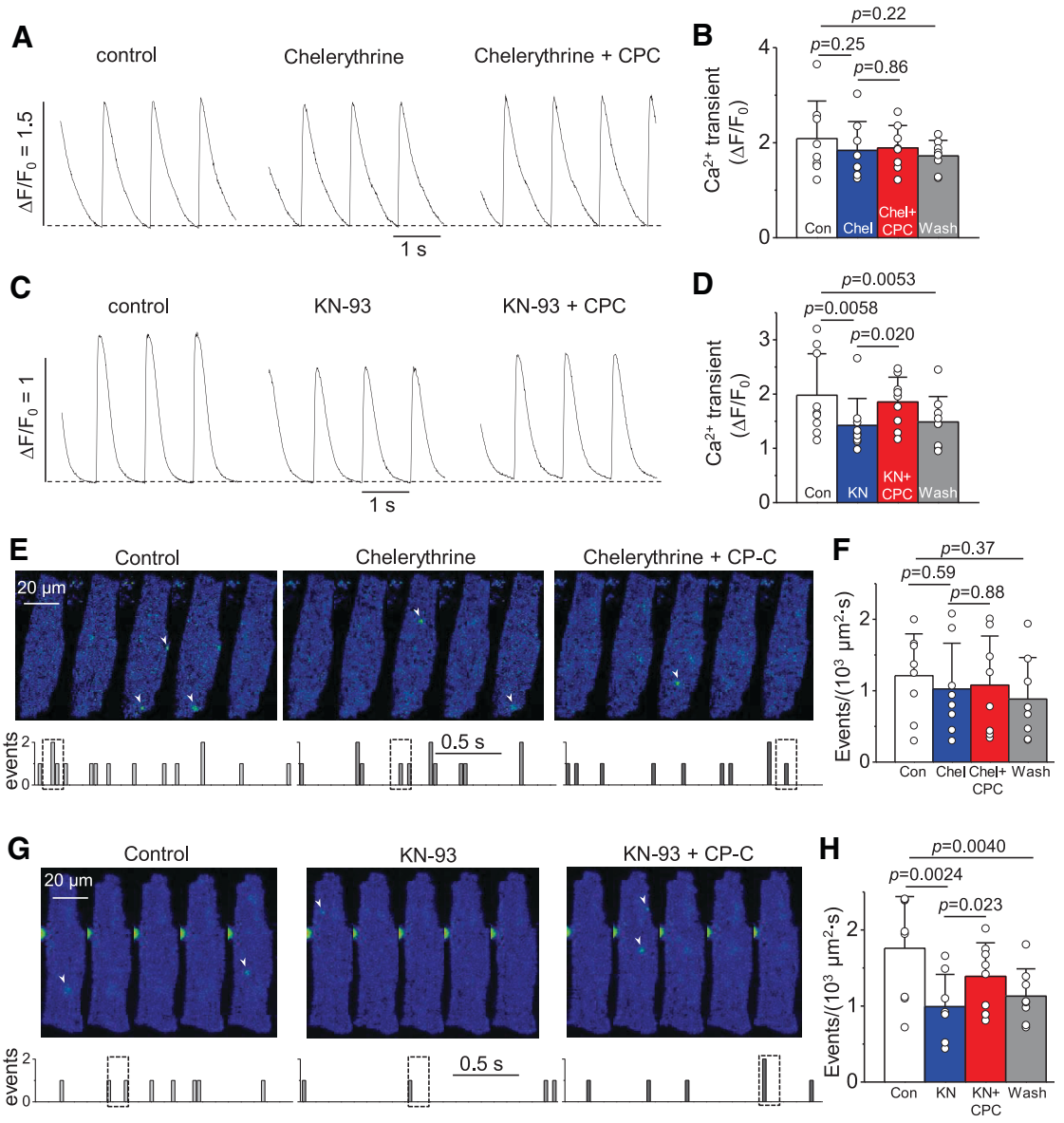

Fig. 6. Major role of PKC in the stimulatory effects by chrysosplenol-C (CP-C) on Ca^{2+} transients and sparks. (A and C) Representative Ca^{2+} transients sequentially recorded in a same rat ventricular myocyte exposed to the PKC inhibitor chelerythrine (2 μM) (A) or 1 μM KN-93, the CaMKII inhibitor (C) followed by additional application of 50 μM CP-C for 3 minutes. (B and D) Summary of the effects of chelerythrine (Chel; $n = 8$, B) or KN-93 (D; $n = 9$) without and with CP-C on the magnitude of Ca^{2+} transients. (E and G) Upper: representative sequential confocal Ca^{2+} images selected during the period marked with boxes in the time courses below each series of images (lower panel) showing spontaneous Ca^{2+} sparks in rat ventricular myocytes in the control solutions and after application of chelerythrine (E; 2 μM) or KN-93 (G; 1 μM) without and with CP-C (50 μM). Arrowheads indicate Ca^{2+} sparks. Lower: time course of spark occurrence during 2-second-long imaging at 30 Hz in the cell shown above. (F and H) Summary of the effects of CP-C in the presence of 2 μM Chel (F; $n = 8$) or 1 μM KN-93 (H; $n = 8$). Considering the new p value after the Bonferroni correction, p value less than 0.017 (0.05/3 paired t tests; equivalent to old 0.05) was considered to be significant. Con, control.

(Fig. 6, E and F). However, in the presence of KN-93, chrysosplenol-C (50 μM) tended to increase the spark occurrence (by 32 ± 5.2%, $n = 8$; Fig. 6, G and H). It should be noted that the effect of chrysosplenol-C on the spark frequency was smaller in the presence of KN-93 compared with that under control conditions (compare with Fig. 3B; $P < 0.01$). These results suggest that PKC may play a key role in the enhancement of spark frequency and Ca^{2+} transients in the presence of chrysosplenol-C and that CaMKII may also partly contribute to the enhancement of Ca^{2+} transients and sparks under the control of PKC.

Next, we confirmed whether chrysosplenol-C–induced positive inotropic effect is mediated by PKC in rat ventricular myocytes. The application of chrysosplenol-C increased cell shortening by ~2-fold at the concentrations of 50 μM (Fig. 7A). This chrysosplenol-C–mediated positive inotropic effect was completely removed by preincubation of either chelerythrine or GF109203X, which are PKC inhibitors (Fig. 7, D and G). Consistent with the Ca^{2+} data, the pretreatment of KN-93 (1 μM) tended to suppress the positive inotropic effect of chrysosplenol-C (Fig. 7, B and G), whereas its inactive analog KN-92 did not suppress the chrysosplenol-C–induced positive inotropic effect (Fig. 7, C and G).

TABLE 1
Effects of KN-93 or chelerythrine on diastolic Ca^{2+} level and transient decay time constant in the absence and presence of chrysosplenol-C in rat ventricular myocytes
Data represent mean ± S.D. The number in the parenthesis indicates number of cells. Paired t tests were done. Considering the new p value after the Bonferroni correction, p value less than 0.0125 (0.05/4) was considered to be significant.

	Diastolic $[Ca^{2+}]$ (F/F_0)	Decay (τ, ms)	n
Control	1	156 ± 52	12
KN-93	1.02 ± 0.0045	160 ± 51	12
KN-93 + CP-C	1.07 ± 0.026*	162 ± 76	12
Control	1	165 ± 34	8
Chel	1.06 ± 0.013	168 ± 44	8
Chel + CP-C	1.05 ± 0.018	169 ± 54	8

Chel, chelerythrine (2 μM); CP-C. chrysosplenol-C.

KN-93 itself but not KN-92 slightly reduced cell shortening with no significance (Fig. 7, B and C), which is somewhat consistent with its effect on Ca^{2+} transients (Fig. 6C). The inhibition of phospholipase C (PLC), which generates the PKC substrate diacylglycerol and inositol 1,4,5-trisphosphate, using U73122 did not significantly attenuate chrysosplenol-C–mediated positive inotropic effect (Fig. 7, E and G). Its inactive analog U73343 also showed no significant effect on the chrysosplenol-C–induced positive inotropy (Fig. 7, F and G), although both chemicals tended to decrease contraction. These results support the major role of PKC in chrysosplenol-C–induced positive inotropy.

The next experiments were designed to determine whether chrysosplenol-C alters the activity of PKC in these myocytes. For this purpose, we examined the effects of chrysosplenol-C on the subcellular distribution of individual PKC isoforms. Immunoblot analyses with antibodies that detect the three major PKC isoforms (PKC-α, PKC-δ, and PKC-ε) expressed in rat ventricular myocytes (Goldberg et al., 1997; Simonis et al., 2002) were performed on cytosolic and membrane fractions of rat ventricular myocytes. The membrane fraction was further divided into Triton-soluble and Triton-insoluble membrane components because scaffolding proteins that play an important role in signal transduction are known to be generally Triton-insoluble (Yan et al., 1996; Anderson, 1998). We confirmed the subcellular fractions by detecting well known cytosolic and membrane markers, GAPDH and Na^+-K^+ ATPase, respectively, using immunoblotting (Fig. 8). Figure 8 demonstrates that PKC-α and PKC-δ preferentially partition to the insoluble membrane fractions from 2 minutes to 5 minutes after exposure to chrysosplenol-C (80 μM). Note that the level of PKC-δ in the insoluble membrane increased earlier compared with that of PKC-α and was maximized at 2 minutes after the drug exposure. The partition of PKC-α in the soluble membrane fraction was prominent after 30-minute exposure to chrysosplenol-C with a gradual decrease in the level of cytosolic PKC-α (Fig. 8A), although the signal changes were not statistically significant (Fig. 8C). The level of PKC-δ in the soluble membrane was also increased from 2 minutes to 5 minutes after exposure to the drug (Fig. 8, A and C). The expression of PKC-ε was detected in the soluble and membrane fractions, but the partition of PKC-ε in the membrane fractions was not observed after the treatment of chrysosplenol-C (Fig. 8, B and C). This result suggests that the activity of PKC-α and PKC-δ increases after chrysosplenol-C treatment. The time course of redistribution of each isoform suggests that PKC-δ may play a role in chrysosplenol-C–induced positive inotropy.

Discussion

Our data provide a cellular mechanism for the previously reported positive inotropy by chrysosplenol-C in rat ventricular myocytes. We found that chrysosplenol-C increases Ca^{2+} transient magnitude (Fig. 1) with no change in Ca^{2+} influx through the L-type Ca^{2+} channel (Fig. 2) and that this chemical enhances resting Ca^{2+} spark occurrence and spark amplitude and duration with a significant increase in the SR Ca^{2+} content (Figs. 3–5). The stimulatory effects of chrysosplenol-C on Ca^{2+} transients and Ca^{2+} sparks were eliminated by PKC inhibition and partially suppressed by CaMKII suppression (Fig. 6). Consistently, the blockade of PKC abolished chrysosplenol-C–induced positive inotropic effects (Fig. 7). Pharmacological data suggested that PLC may not play a role in the positive inotropic effect exerted by chrysosplenol-C (Fig. 7). Immunoblotting in the subcellular fractions of rat ventricular myocytes demonstrated significant translocation/activation of PKC-δ by chrysosplenol-C with a time course similar to that of the positive inotropic effect (time-to-peak effect = 2 minutes; Son et al., 2011) and a delayed PKC-α translocation to the membrane fractions (Fig. 8). Our data suggest that chrysosplenol-C may elicit a positive inotropic effect by enhancing SR Ca^{2+} releases on depolarizations with increasing SR Ca^{2+} loading via the activation of specific PKC isoform independently of PLC.

It is well known that enhancements of resting Ca^{2+} spark occurrence depend on SR Ca^{2+} loading (Satoh et al., 1997). Larger SR Ca^{2+} loading in chrysosplenol-C–treated myocytes compared with cells under control conditions (Fig. 5) may explain the increased Ca^{2+} spark frequency as well as the larger sparks observed in the presence of chysosplenol-C (Fig. 4). Due to larger Ca^{2+} loading in the SR in the presence of chrysosplenol-C, Ca^{2+} release on depolarizations may also increase (Cheng et al., 1993; Bassani et al., 1995; Satoh et al., 1997). Previous reports support the notion that SR Ca^{2+} load correlates with Ca^{2+}-induced Ca^{2+} release gain function in cardiac myocytes (Cheng et al., 1993; Bassani et al., 1995). Although both depolarization-induced Ca^{2+} release and SR Ca^{2+} content were increased by chrysosplenol-C, the fractional Ca^{2+} release was not altered (Fig. 5B). This result also supports the notion that the stimulatory effects of chrysosplenol-C on Ca^{2+} releases involve a mode of action distinct from β_1-adrenergic signaling (Son et al., 2011) because β_1-adrenergic stimulation augments the fractional release as well as SR Ca^{2+} content (Ginsburg and Bers, 2004). Consistently, neither the decay of Ca^{2+} transient nor I_{Ca} was significantly altered in the presence of chrysosplenol-C (Figs. 1 and 2).

It should be noted that fractional Ca^{2+} release measured as intracellular total Ca^{2+} concentrations would be slightly different from that assessed as free Ca^{2+} concentrations (Bassani et al., 1995). We estimated fractional release by the measurements of cytosolic free Ca^{2+} using a nonlinear Ca^{2+} indicator (fluo-4) as previously reported (Kim et al., 2015). It is suggested that Ca^{2+} buffering power decreases with increasing intracellular Ca^{2+} level (Eisner et al., 2000). Therefore, given that the caffeine-evoked rise is larger than that produced by electrical stimulation, a bigger effect of intracellular Ca^{2+} buffering at lower Ca^{2+} concentrations would have caused underestimation of the fractional release under drug stimulation. Nevertheless, using the current

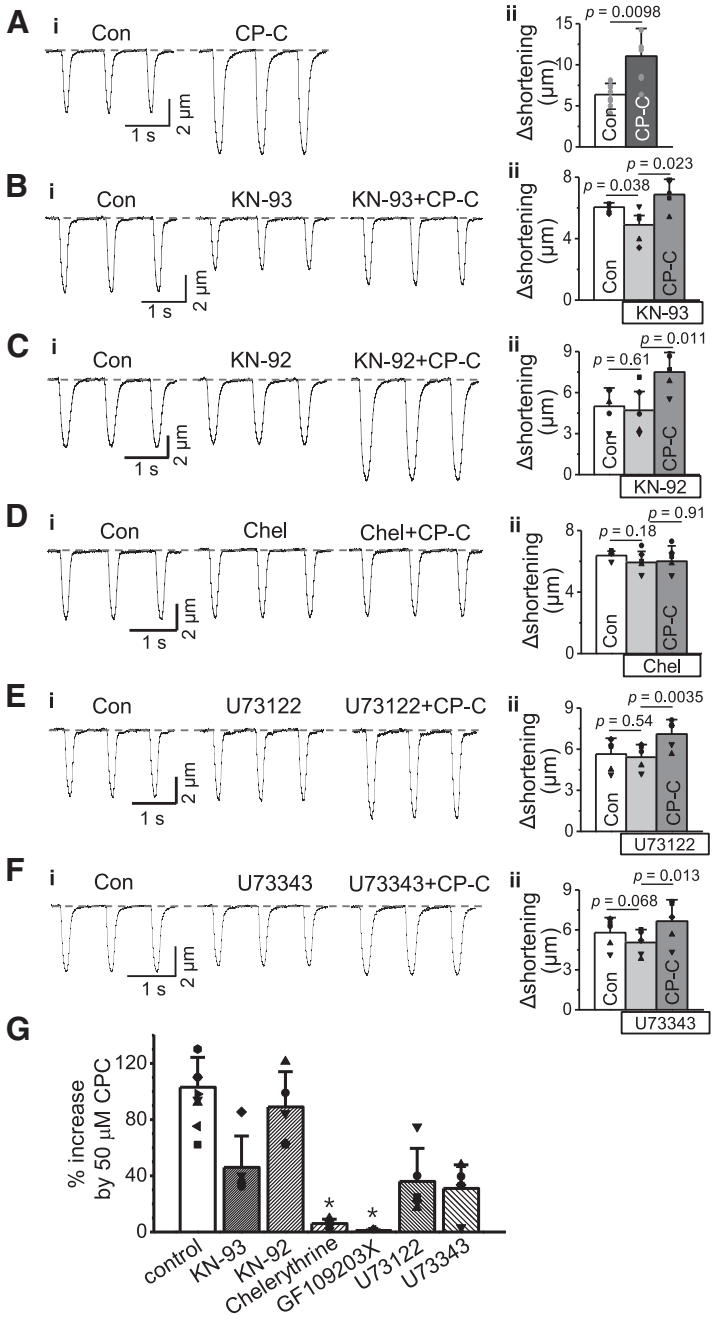

Fig. 7. Role of PKC in chrysosplenol-C–induced positive inotropy in rat ventricular myocytes. Chrysosplenol-C (CP-C) (50 μM)-induced positive inotropic effects under control conditions (A) and their modulations in cells pretreated with KN-93 (1 μM, 6 minutes), the CaMKII inhibitor (B), KN-92 (1 μM, 6 minutes), the inactive analog of KN-93 (C), chelerythrine (D; 2 μM, Chel), PLC inhibitor (E; 5 μM U73122), or U73343, the inactive analog of U73122 (F; 5 μM U73343). *i* shows representative cell shortening traces recorded before (Con) and after each drug effect became stable. *ii* represents mean magnitude of cell shortening measured before and after the applications of CP-C in the absence (A; $n = 8$) and presence of KN-93 (B; $n = 5$), KN-92 (C; $n = 5$), chelerythrine (D; $n = 5$), U73122 (E; $n = 6$), or U73343 (F; $n = 5$), (B), KN-92 (C), U73122 (E), or U73343 (F) (paired t test). (G) Comparison of mean % increases in cell shortening by 50 μM CP-C between control conditions and interventions indicated. GF109203X: 5 μM ($n = 6$). Considering the new p value after the Bonferroni correction (0.05/6 = 0.0083), % change in contraction by CP-C was significantly different in the presence of chelerythrine and GF109203X compared with that under control condition (*).

method, we have successfully observed the enhancement of fractional release by another positive inotropic agent murrayafoline-A that distinctly increases I_{Ca}, SR Ca^{2+} content, and the sensitivity of Ca^{2+} release sites (Kim et al., 2015).

Since SR Ca^{2+} loading was increased with no significant acceleration of Ca^{2+} transient decay in the presence of chrysosplenol-C, larger SR Ca^{2+} loading may be due to increased Ca^{2+} entry and reduced Ca^{2+} removal across the cell membrane. The decay rate of caffeine-induced Ca^{2+} transient that reflects the activity of forward mode Na^+-Ca^{2+} exchanger was not altered by chrysosplenol-C (Fig. 5B). In this regard, we have observed that the removal of external Na^+ and Ca^{2+} suppressed the chrysosplenol-C–mediated increase in the resting spark frequency (Q.A.Le and S.H.Woo, unpublished observations). This suggests that the Na^+ and Ca^{2+} transporter/channels in the cell membrane may be modulated by chrysosplenol-C–PKC signaling.

In fact, large SR Ca^{2+} leaks can result in a decrease in SR Ca^{2+} content. However, the maximal effect of chrysosplenol-C on the Ca^{2+} spark frequency was ~1.7–1.8 fold only, and chrysosplenol-C did not dramatically increase diastolic Ca^{2+} levels (Fig. 1). This mild increase in the resting Ca^{2+} spark occurrence is in contrast with the effect of isoproterenol, which increases spark frequency in ventricular myocytes by ~5-fold (Potenza et al., 2019). It should be noted that because chrysosplenol-C increases cytosolic Ca^{2+} and SR Ca^{2+} loading, it could generate adverse effects, such as arrhythmias, due to intracellular Ca^{2+} overload, as other Ca^{2+} mobilizing positive inotropic

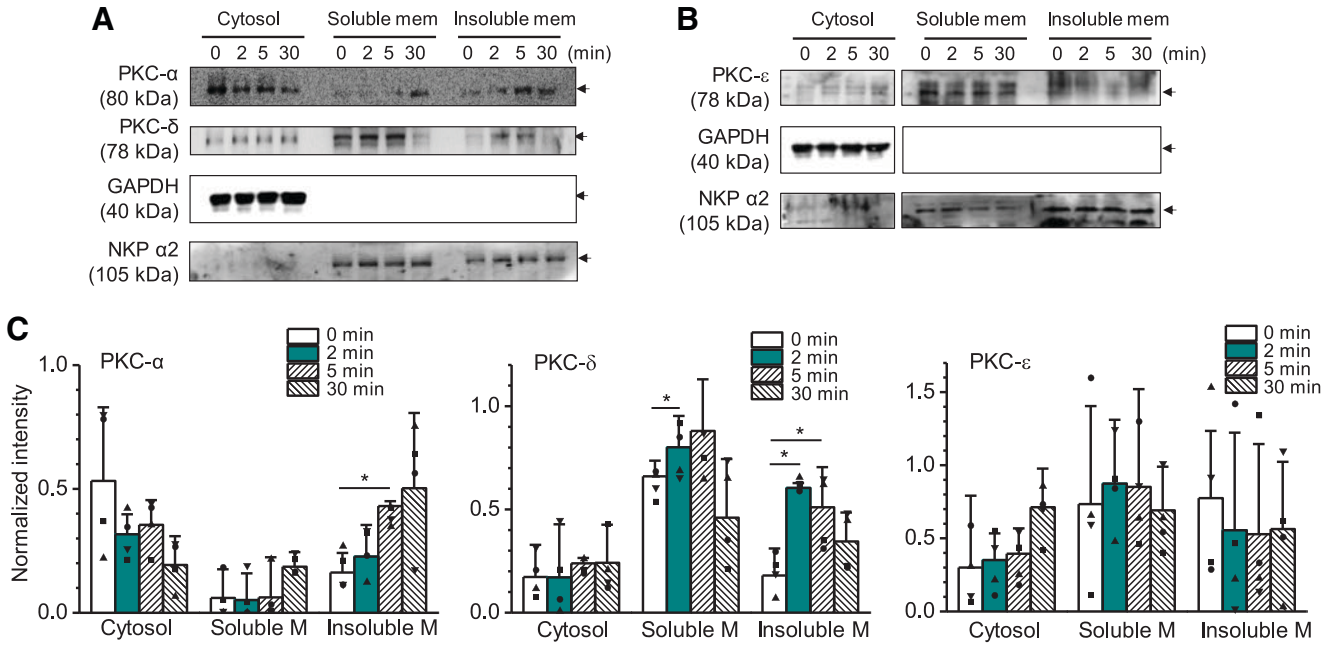

Fig. 8. Redistributions of PKC subtypes by the treatment of chrysosplenol-C in rat ventricular myocytes. (A and B) Western blots with antibodies specific for PKC-α (A), PKC-δ (A), and PKC-ε (B) using cytosolic and particulate fractions [soluble membrane (mem, M) and insoluble membrane] of rat ventricular myocytes treated with control solutions and with 80 μM chrysosplenol-C for 2, 5, and 30 minutes. As a standard for cytosolic protein and membrane protein, GAPDH and Na^+-K^+ pump (NKP) were used, respectively. (C) Relative quantification of each PKC subtype Western bands (A and B) compared with standard protein expression (GAPDH or NKP). Four rats (four Western blotting) were used. Two-way ANOVA–related measures with post hoc testing to control for multiple comparisons were used to test statistical significance (*). Namely, each ANOVA was run at a new p value of 0.05/3 (0.017).

agents (e.g., isoproterenol and digitalis) showed (Vassalle and Lin, 2004; Steinberg, 2018). In this regard, CaMKII that appears to be secondarily activated by PKC activity (Figs. 6 and 7) may induce SR Ca^{2+} leak (Tani, 1990), thereby contributing to arrhythmogenesis.

Our findings indicate that PKC may play a key role in the chrysosplenol-C–induced positive inotropic effect by enhancing SR Ca^{2+} releases in ventricular myocytes. In fact, there are significant differences in the inotropic responses under various first messengers (agonist/hormones) to activate PKC or PKC activators in terms of time course and effects. Involvement of PKC in the biphasic inotropic responses of cardiac myocytes has been previously reported under the stimulations of the endothelin receptor and α_1-adrenergic receptor, although there have been controversial findings depending on species and experimental conditions (Capogrossi et al., 1991; Woo and Lee, 1999a,b; O-Uchi et al., 2008; Smyrnias et al., 2018). Direct activation of PKC using phorbol 12-myristate 13-acetate has also induced positive inotropic effects and enhanced Ca^{2+} transients and I_{Ca} in cardiac myocytes, but there were other inconsistent observations (decrease or no change) depending on the species and experimental conditions (Lacerda et al., 1988; Walsh and Kass, 1988; Capogrossi et al., 1990; MacLeod and Harding, 1991; Tseng and Boyden, 1991; Woo and Lee, 1999b). The positive inotropic effects of these stimulations appeared to be related to mild enhancement of Ca^{2+} release and Ca^{2+} current. In case of the effect of chrysosplenol-C, PKC does not seem to alter I_{Ca}. Diverse effects of PKC under different agonists in cardiac myocytes may be caused by differences in the PKC isoforms involved and compartmentalization of relevant signaling molecules within the cells. According to our results, translocation of PKC-δ to the membrane fractions was the most prominent after 2 minutes of the chrysosplenol-C exposure (Fig. 8) when we normally observed maximal stimulatory effects on contraction (Son et al., 2011), Ca^{2+} transients, and sparks. Therefore, it is plausible to think that this isoform mediates the positive inotropic effect of chrysosplenol-C. There was a difference in the redistribution patterns between the soluble and insoluble membrane fractions of PKC-α and PKC-δ. PKC-α increased in the insoluble membrane after 5 minutes with a gradual decrease in its level in the cytosolic fraction, whereas PKC-δ was increased in both soluble and insoluble membrane fractions for 5 minutes with no significant reduction in its level in the cytosolic fractions (Fig. 8). It is known that various signaling molecules, including mitogen-activated protein kinases, extracellular signal-regulated kinases, and scaffolding proteins in the t-tubules, caveolae, and cytoskeleton are known to be contained in the Triton-insoluble membrane fraction in cardiac myocytes (Yan et al., 1996; Anderson, 1998; Ballard-Croft et al., 2008). Partitions of PKC-α and -δ into the insoluble membrane fractions suggest that interaction between the PKC isoforms and signaling molecules in those subcellular compartments.

Previous reports of the heart from PKC-α knockout mice, PKC-α–overexpressing mice, and cardiac cells with adenoviral PKC-α knockdown suggest that PKC-α reduces cardiac contraction via lowering Ca^{2+} transient and Ca^{2+} loading in the SR (Braz et al., 2004). Regarding the role of PKC-δ in cardiac contraction regulation, it has been demonstrated in myocytes expressing PKC-δ-GFP that phorbol dibutyrate (PDBu), the PKC activator, caused a transient negative inotropic response followed by a robust and sustained positive inotropic response that paralleled PKC-δ accumulation in the Golgi and other subcellular domain (Kang and Walker, 2005). The

cardiac cells expressing PKC-ε–GFP also showed similar stimulatory effects by PDBu on contraction (Kang and Walker, 2005). The PKC-ε, however, has been shown to mediate endothelin-1–induced negative inotropy in rat ventricular myocytes (Smyrnias et al., 2018). In addition, the PDBu-induced negative inotropic response has been suggested to be mediated by PKC-α (Kang and Walker, 2005). This previous evidence appears to be consistent with our hypothesis that PKC-δ that was early partitioned by chrysosplenol-C to the soluble and insoluble membrane may be responsible for the positive inotropy. Such hypothesis warrants further investigations.

Authorship Contributions

Participated in research design: Woo.

Conducted experiments: Wang, Trinh, Vu, Ohk, Zhang.

Contributed new reagents or analytic tools: Hoang, Nguyen.

Performed data analysis: Wang, Trinh, Kim, Woo.

Wrote or contributed to the writing of the manuscript: Wang, Trinh, Vu, Kim, Woo.

References

Anderson RGW (1998) The caveolae membrane system. *Annu Rev Biochem* **67**:199–225.

Asai T, Shuba LM, Pelzer DJ, and McDonald TF (1996) PKC-independent inhibition of cardiac L-type Ca^{2+} channel current by phorbol esters. *Am J Physiol* **270**:H620–H627.

Ballard-Croft C, Locklar AC, Keith BJ, Mentzer Jr RM, and Lasley RD (2008) Oxidative stress and adenosine A_1 receptor activation differentially modulate subcellular cardiomyocyte MAPKs. *Am J Physiol Heart Circ Physiol* **294**:H263–H271.

Bassani JWM, Bassani RA, and Bers DM (1994) Relaxation in rabbit and rat cardiac cells: species-dependent differences in cellular mechanisms. *J Physiol* **476**:279–293.

Bassani JWM, Yuan W, and Bers DM (1995) Fractional SR Ca release is regulated by trigger Ca and SR Ca content in cardiac myocytes. *Am J Physiol* **268**:C1313–C1319.

Beuckelmann DJ and Wier WG (1988) Mechanism of release of calcium from sarcoplasmic reticulum of guinea-pig cardiac cells. *J Physiol* **405**:233–255.

Bovo E, Huke S, Blatter LA, and Zima AV (2017) The effect of PKA-mediated phosphorylation of ryanodine receptor on SR Ca^{2+} leak in ventricular myocytes. *J Mol Cell Cardiol* **104**:9–16.

Braz JC, Gregory K, Pathak A, Zhao W, Sahin B, Klevitsky R, Kimball TF, Lorenz JN, Nairn AC, Liggett SB, et al. (2004) PKC-alpha regulates cardiac contractility and propensity toward heart failure. *Nat Med* **10**:248–254.

Cannell MB, Cheng H, and Lederer WJ (1994) Spatial non-uniformities in $[Ca^{2+}]_i$ during excitation-contraction coupling in cardiac myocytes. *Biophys J* **67**:1942–1956.

Capogrossi MC, Kaku T, Filburn CR, Pelto DJ, Hansford RG, Spurgeon HA, and Lakatta EG (1990) Phorbol ester and dioctanoylglycerol stimulate membrane association of protein kinase C and have a negative inotropic effect mediated by changes in cytosolic Ca^{2+} in adult rat cardiac myocytes. *Circ Res* **66**:1143–1155.

Capogrossi MC, Kachadorian WA, Gambassi G, Spurgeon HA, and Lakatta EG (1991) Ca^{2+} dependence of α-adrenergic effects on the contractile properties and Ca^{2+} homeostasis of cardiac myocytes. *Circ Res* **69**:540–550.

Cheng H, Lederer WJ, and Cannell MB (1993) Calcium sparks: elementary events underlying excitation-contraction coupling in heart muscle. *Science* **262**:740–744.

Eisner DA, Choi HS, Díaz ME, O'Neill SC, and Trafford AW (2000) Integrative analysis of calcium cycling in cardiac muscle. *Circ Res* **87**:1087–1094.

Ginsburg KS and Bers DM (2004) Modulation of excitation-contraction coupling by isoproterenol in cardiomyocytes with controlled SR Ca^{2+} load and Ca^{2+} current trigger. *J Physiol* **556**:463–480.

Goldberg M, Zhang HL, and Steinberg SF (1997) Hypoxia alters the subcellular distribution of protein kinase C isoforms in neonatal rat ventricular myocytes. *J Clin Invest* **99**:55–61.

Guo T, Zhang T, Mestril R, and Bers DM (2006) Ca^{2+}/calmodulin-dependent protein kinase II phosphorylation of ryanodine receptor does affect calcium sparks in mouse ventricular myocytes. *Circ Res* **99**:398–406.

Györke I and Györke S (1998) Regulation of the cardiac ryanodine receptor channel by luminal Ca^{2+} involves luminal Ca^{2+} sensing sites. *Biophys J* **75**:2801–2810.

Hamill OP, Marty A, Neher E, Sakmann B, and Sigworth FJ (1981) Improved patch-clamp techniques for high-resolution current recording from cells and cell-free membrane patches. *Pflugers Arch* **391**:85–100.

Han S, Schiefer A, and Isenberg G (1994) Ca^{2+} load of guinea-pig ventricular myocytes determines efficacy of brief Ca^{2+} currents as trigger for Ca^{2+} release. *J Physiol* **480**: 411–421.

Huong DT, Kamperdick C, and Sung TV (2004) Homogentisic acid derivatives from *Miliusa balansae*. *J Nat Prod* **67**:445–447.

Janczewski AM, Spurgeon HA, Stern MD, and Lakatta EG (1995) Effects of sarcoplasmic reticulum Ca^{2+} load on the gain function of Ca^{2+} release by Ca^{2+} current in cardiac cells. *Am J Physiol* **268**:H916–H920.

Kang M and Walker JW (2005) Protein kinase C delta and epsilon mediate positive inotropy in adult ventricular myocytes. *J Mol Cell Cardiol* **38**:753–764.

Kim JC, Wang J, Son MJ, Cuong NM, and Woo SH (2015) Sensitization of cardiac Ca^{2+} release sites by protein kinase C signaling: evidence from action of murrayafoline A. *Pflugers Arch* **467**:1607–1621.

Lacerda AE, Rampe D, and Brown AM (1988) Effects of protein kinase C activators on cardiac Ca^{2+} channels. *Nature* **335**:249–251.

Lu S, Liao Z, Lu X, Katschinski DM, Mercola M, Chen J, Heller Brown J, Molkentin JD, Bossuyt J, and Bers DM (2020) Hyperglycemia acutely increases cytosolic reactive oxygen species via O-linked GlcNAcylation and CaMKII activation in mouse ventricular myocytes. *Circ Res* **126**:e80–e96.

MacLeod KT and Harding SE (1991) Effects of phorbol ester on contraction, intracellular pH and intracellular Ca^{2+} in isolated mammalian ventricular myocytes. *J Physiol* **444**:481–498.

Maier LS and Bers DM (2007) Role of Ca^{2+}/calmodulin-dependent protein kinase (CaMK) in excitation-contraction coupling in the heart. *Cardiovasc Res* **73**:631–640.

Näbauer M, Callewaert G, Cleemann L, and Morad M (1989) Regulation of calcium release is gated by calcium current, not gating charge, in cardiac myocytes. *Science* **244**:800–803.

Negretti N, O'Neill SC, and Eisner DA (1993) The relative contributions of different intracellular and sarcolemmal systems to relaxation in rat ventricular myocytes. *Cardiovasc Res* **27**:1826–1830.

Niggli E and Lederer WJ (1990) Voltage-independent calcium release in heart muscle. *Science* **250**:565–568.

Ogrodnik J and Niggli E (2010) Increased $Ca^{(2+)}$ leak and spatiotemporal coherence of $Ca^{(2+)}$ release in cardiomyocytes during β-adrenergic stimulation. *J Physiol* **588**:225–242.

O-Uchi J, Sasaki H, Morimoto S, Kusakari Y, Shinji H, Obata T, Hongo K, Komukai K, and Kurihara S (2008) Interaction of alpha1-adrenoceptor subtypes with different G proteins induces opposite effects on cardiac L-type Ca^{2+} channel. *Circ Res* **102**:1378–1388.

Pereira L, Métrich M, Fernández-Velasco M, Lucas A, Leroy J, Perrier R, Morel E, Fischmeister R, Richard S, Bénitah JP, et al. (2007) The cAMP binding protein Epac modulates Ca2+ sparks by a Ca2+/calmodulin kinase signalling pathway in rat cardiac myocytes. *J Physiol* **583**:685–694.

Potenza DM, Janicek R, Fernandez-Tenorio M, Camors E, Ramos-Mondragón R, Valdivia HH, and Niggli E (2019) Phosphorylation of the ryanodine receptor 2 at serine 2030 is required for a complete β-adrenergic response. *J Gen Physiol* **151**: 131–145.

Puglisi JL, Yuan W, Timofeyev V, Myers RE, Chiamvimonvat N, Samarel AM, and Bers DM (2011) Phorbol ester and endothelin-1 alter functional expression of Na^+/Ca^{2+} exchange, K^+, and Ca^{2+} currents in cultured neonatal rat myocytes. *Am J Physiol Heart Circ Physiol* **300**:H617–H626.

Satoh H, Blatter LA, and Bers DM (1997) Effects of $[Ca^{2+}]_i$, SR Ca^{2+} load, and rest on Ca^{2+} spark frequency in ventricular myocytes. *Am J Physiol* **272**:H657–H668.

Semple SJ, Nobbs SF, Pyke SM, Reynolds GD, and Flower RL (1999) Antiviral flavonoid from Pterocaulon sphacelatum, an Australian Aboriginal medicine. *J Ethnopharmacol* **68**:283–288.

Shacklock PS, Wier WG, and Balke CW (1995) Local Ca^{2+} transients (Ca^{2+} sparks) originate at transverse tubules in rat heart cells. *J Physiol* **487**:601–608.

Simonis G, Honold J, Schwarz K, Braun MU, and Strasser RH (2002) Regulation of the isozymes of protein kinase C in the surviving rat myocardium after myocardial infarction: distinct modulation for PKC-alpha and for PKC-delta. *Basic Res Cardiol* **97**:223–231.

Smyrnias I, Goodwin N, Wachten D, Skogestad J, Aronsen JM, Robinson EL, Demydenko K, Segonds-Pichon A, Oxley D, Sadayappan S, et al. (2018) Contractile responses to endothelin-1 are regulated by PKC phosphorylation of cardiac myosin binding protein-C in rat ventricular myocytes. *J Mol Cell Cardiol* **117**:1–18.

Son MJ, Kim HK, Huong TT, Kim YH, Van Sung T, Cuong NM, and Woo SH (2011) Chrysosplenol C increases contraction in rat ventricular myocytes. *J Cardiovasc Pharmacol* **57**:259–262.

Steinberg SF (2018) β1-adrenergic receptor regulation revisited. *Circ Res* **123**:1199–1201.

Tani M (1990) Mechanisms of Ca^{2+} overload in reperfused ischemic myocardium. *Annu Rev Physiol* **52**:543–559.

Tseng GN and Boyden PA (1991) Different effects of intracellular Ca and protein kinase C on cardiac T and L Ca currents. *Am J Physiol* **261**:H364–H379.

Vassalle M and Lin CI (2004) Calcium overload and cardiac function. *J Biomed Sci* **11**:542–565.

Walsh KB and Kass RS (1988) Regulation of a heart potassium channel by protein kinase A and C. *Science* **242**:67–69.

Waxham MN and Aronowski J (1993) Ca^{2+}/calmodulin-dependent protein kinase II is phosphorylated by protein kinase C in vitro. *Biochemistry* **32**:2923–2930.

Woo SH and Lee CO (1999a) Effects of endothelin-1 on Ca^{2+} signaling in guinea-pig ventricular myocytes: role of protein kinase C. *J Mol Cell Cardiol* **31**:631–643.

Woo SH and Lee CO (1999b) Role of PKC in the effects of α1-adrenergic stimulation on Ca^{2+} transients, contraction and Ca^{2+} current in guinea-pig ventricular myocytes. *Pflugers Arch* **437**:335–344.

Woo SH, Cleemann L, and Morad M (2003) Spatiotemporal characteristics of junctional and nonjunctional focal Ca^{2+} release in rat atrial myocytes. *Circ Res* **92**:e1–e11.

Yan SR, Fumagalli L, and Berton G (1996) Activation of SRC family kinases in human neutrophils. Evidence that p58C-FGR and p53/56LYN redistributed to a Triton X-100-insoluble cytoskeletal fraction, also enriched in the caveolar protein caveolin, display an enhanced kinase activity. *FEBS Lett* **380**:198–203.

Zhou P, Zhao YT, Guo YB, Xu SM, Bai SH, Lakatta EG, Cheng H, Hao XM, and Wang SQ (2009) β-adrenergic signaling accelerates and synchronizes cardiac ryanodine receptor response to a single L-type Ca^{2+} channel. *Proc Natl Acad Sci USA* **106**:18028–18033.

Address correspondence to: Sun-Hee Woo, Chungnam National University, 99 Daehak-ro, Daejeon, South Korea. E-mail: shwoo@cnu.ac.kr